

The 2014A Report

April 1, 2014

The DIVING^{3D} project: Deep IFS View of Nuclei of Galaxies

J. E. Steiner¹, R. Cid Fernandes², P. Coelho¹, N. Vale Asari², R. B. Menezes¹, T. V. Ricci¹, D. May¹ & A. L. de Amorim²

¹Instituto de Astronomia, Geofísica e Ciências Atmosféricas, Universidade de São Paulo, Rua do Matão 1226, Cidade Universitária, São Paulo, SP CEP 05508-090, Brazil

²Departamento de Física, Universidade Federal de Santa Catarina, PO Box 476, 88040-900, Florianópolis, SC, Brazil

Executive summary

Introduction

The legacy strategy

The massive galaxies subsample

The late type galaxies subsample

Relevant publications

Appendix A- List of all galaxies of the project

Appendix B- List of galaxies with nuclear activity

Appendix C- The original proposal

Executive Summary

This is the first (2014A) report of the project approved in the Brazilian LLP (Large and Long Project program) **DIVING^{3D}: Deep IFS View of Nuclei of Galaxies** (formerly GSGN – Gemini Survey of Galactic Nuclei).

In this report we present a preliminary analysis of two previous subsamples of galaxies that have been observed with the GMOS: 1- the massive galaxy subsample and 2- the late type galaxy subsample. We also provide answers to questions posed by the NTAC. A total of 47 galaxies have already been observed, representing 28% of the total of 170 galaxies of the complete project.

The observations of the massive galaxies ($\sigma > 200$ km/s) subsample have been completed on Dec 24, 2013. A total of 35 galaxies have been observed. All galaxies were already submitted to two phases: a- data reduction (wavelength and flux calibration and DAR correction); b- data processing (fingerprint removal, spatial Butterworth filtering and Richardson-Lucy deconvolution). PCA Tomography has been provided and a preliminary statistical analysis is given. We found that in, our sample, that at least 43% of all galaxies have a broad H α component. We also found that 69% present circumnuclear emission lines and at least 26%, ionization cones. We also found that 69% of the galactic cores are fast rotators while 31% are slow rotators.

In the next step, we will perform stellar spectral synthesis in order to refine the analysis and produce data cubes for the gas emission only. This will provide a more reliable quantitative analysis. We have done this already with NGC 3115, a classical S0 galaxy with no emission line previously detected. We found a Seyfert 1 nucleus off centered. A Letter will soon be submitted to the ApJ.

The late type galaxy subsample (Sc-Sd galaxies) is still in the data acquisition phase. Up to now 10 galaxies have been observed. Three of these objects (NGC 300, NGC 1313 and NGC 7424) have already been reduced, processed and analyzed. A brief summary is presented.

A total of $35 + 12 = 47$ galaxies have already been observed (this includes 1 Sab and one Sb galaxy). This represents 28% of the total sample.

Introduction

The LLP project was approved with the name “GSGN –Gemini Survey of Galactic Nuclei”. The group decided to change to a definite name: “The DIVING^{3D} project: Deep IFS View of Nuclei of Galaxies”.

As explained in the initial proposal (section of experimental design), we have chosen all galaxies with $B < 12.0$, $\delta < 0^\circ$ and $|b| > 15^\circ$. This sample has a total of 181 galaxies. From them, 11 are Sm/Im in which one cannot identify a nucleus in the 2MASS images. The total number of our sample is therefore 170 galaxies. We list all galaxies in Appendix A. In appendix B we list all objects known to have AGN, according to the NED-NASA Extragalactic Database. A total of 29 objects are classified in this category, including Seyferts, LINERS, FSRs (Flat Spectrum Radio Source), and two HII nuclei. This means that, excluding the 2 H II regions, 16% of the galaxies have some sort of AGN observed.

The observations of a sub-sample of 35 massive galaxies ($\sigma > 200$ km/s) has already been completed on Christmas-eve, 2013. We also have already been allocated time in 2013 and 2014A for a second sub-sample – the Sc-Sd sub-sample. These observations are still in progress. We have fully reduced and analyzed 3 of these objects.

The Legacy strategy

Our commitment is to deliver the data to the Brazilian Astronomical Community. The idea is to give access to our community not only to the raw data (available after 1 year anyway) but also the reduced and the processed data. For this reason we will deliver two datacubes for each galaxy:

A – One data-cube with all spectra:

- Calibrated in wavelength
- Calibrated in flux
- Corrected for the differential atmospheric refraction (DAR).

B – One additional cube will be available to the community with the additional data processing:

- Fingerprint removed
- High frequency spatial noise remove with Butterworth filter
- Richardson-Lucy deconvolution

The data will be located in the projects’ site (“DIVING3D” in CLOUD-USP) and can be accessed by any Brazilian scientist or student with a password provided under request. The password must be strictly personal and the data cannot be transferred to non Brazilian astronomers.

We plan to deliver 4 data releases, after observations, preliminary analysis and quality control of the first 25%, 50%, 75% and 100% of the data acquired. The first data release will be made by March, 1, 2015.

The sample definition and subsample observing strategy

We are adopting the following strategy of defining subsamples of galaxies:

| Subsample | | Nr of gal. | obs |
|-----------|--|------------|-----|
| 1- | The subsample of massive galaxies – $\sigma > 200$ km/s | 35 | 35 |
| 2- | The subsample of late type galaxies – Sc - Sd with $B < 11.2$ | 16 | 9 |
| 3- | The subsample of bright galaxies – $B > 11.0$ | 43 | 18 |
| 4- | The subsample of ETG(E+S0) with $\sigma < 200$ km/s and $B > 11.0$ | 28 | 0 |
| 5- | The remaining galaxies. | | |

The sub-sample of massive ($\sigma > 200$ km/s) galaxies

The sub-sample of massive galaxies comprises 35 galaxies. The observations have been completed by December 24, 2013. We have done the following steps so far:

- 1- Data cube reduction: wavelength calibration; flux calibration; DAR (differential atmospheric refraction) correction.
- 2- Data cube processing: Fingerprint removal (using PCA Tomography); high spatial frequency noise filtering (using Butterworth filter); Richardson-Lucy deconvolution.

With these data cubes it is possible to perform a preliminary analysis of all objects. The results are given in the table below. It is important to notice that this analysis is essentially qualitative. More quantitative analyses will be made with other techniques. But these are more time consuming and will be made in the near future.

In this preliminary analysis, we found that 1 object (3%) is a Seyfert galaxy, 29 objects (83%) are LINERs, 4 objects have no emission lines and 1 object is still not classified yet.

Perhaps the most important new result is that 15 out of the 35 galaxies have shown a broad H α component (Sy 1 or Lb). This is usually considered a secure prove of the presence of a supermassive black hole. This is, thus, the case of 43% of the sample.

With respect to the presence of a rotating stellar disk, nearly 2/3 of the sample (69%) are fast rotators while 1/3 (31%) are slow rotators.

One of the advantages of this survey is that we can study the circumnuclear emission line properties. We found that 24 objects (69%) show circumnuclear emission; among them, 9 (26%) show evidence of ionization cones.

It is worth mentioning that we found featureless continua in 4 galaxies (11%) while in 21 galaxies (60%) we found evidence of dust.

The list of targets of the massive galaxy sub-sample is the following:

The sub-sample of massive ($\sigma > 200$ km/s) galaxies

| Name | Type | σ | RG 6cmJy | group/clust | AGN? |
|-------------|--------------|----------|----------|-------------|-------|
| Ellipticals | | | | | |
| IC 1459 | E3-4 | 306 | RG: 1.0 | Gr(30) | FSRS |
| IC 4296 | E | 333 | RG 1.6 | | FSRS |
| NGC 584 | E4 | 206 | | | - |
| NGC 720 | E5 | 241 | | | - |
| NGC 1052 | E4 | 207 | RG | For clust | FSRS |
| NGC 1395 | E2 | 245 | | | - |
| NGC 1399 | cD | 346 | RG 0.34 | | |
| NGC 1404 | E1 | 234 | | | |
| NGC 1407 | E0 | 271 | | | |
| NGC 1549 | E0-1 | 202 | | | |
| NGC 1700 | E4 | 238 | | | |
| NGC 2974 | E4 | 238 | | | Sy 2 |
| NGC 3557 | E3 | 268 | RG 0.30 | | FSRS |
| NGC 3585 | E6 | 206 | | | |
| NGC 3904 | E2-3? | 205 | | Cen clust | |
| NGC 3923 | E4-5 | 257 | | | |
| NGC 3962 | E1 | 233 | | | |
| NGC 4105 | E3 | 262 | | | |
| NGC 4696 | cD | 254 | RG 1.39 | | Liner |
| NGC 5018 | E3? | 210 | | | |
| NGC 5044 | E0 | 242 | | | |
| NGC 6868 | E2 | 255 | 0.12 | | FSRS |
| NGC 7507 | E0 | 222 | | | |
| S0 | | | | | |
| NGC 1316 | SAB0^0(s) | 228 | RG 100 | For A | |
| NGC 1332 | S0^-(s) | 321 | | Eri cl | |
| NGC 1380 | SA0 | 218 | | | |
| NGC 1574 | SA0^-(s)? | 210 | | | |
| NGC 2217 | (R)SB0+(rs) | 203 | | | |
| NGC 2784 | SA0^0(s)? | 225 | | | |
| NGC 3115 | S0^- | 267 | | | |
| NGC 5101 | (R)SB0/a(rs) | 203 | | | |
| NGC 7049 | SA0^0(s) | 246 | 0.035 | | |
| Spirals | | | | | |
| NGC 1300 | SB(rs)bc | 218 | | | |
| NGC 4594 | SA(s)a | 241 | | | Sy 2 |
| NGC 4699 | SAB(rs)b | 215 | | | |

23 E + 9 S0 + 3 S = 35 galaxies with $\sigma > 200$ km/s

The sub-sample of massive ($\sigma > 200$ km/s) galaxies

Preliminary results

| Name | AGN | | Stl.disk | Dust | Comment |
|--------------------|---------|---------|----------|---------------------------|----------------------------------|
| Ellipticals | | | | | |
| IC 1459 | Lb FC | cne | FR | Dust lane (HST) | |
| IC 4296 | Lb | cne IC | SR | Dust lane (HST) | |
| NGC 584 | Lb? | cne | FR | | |
| NGC 720 | Lw | cne | SR | | |
| NGC 1052 | Lb FC | cne | FR | | |
| NGC 1395 | L | cne | FR | | |
| NGC 1399 | *Lw | - | SR | | |
| NGC 1404 | *Lw | - | SR | Dust spot (HST; Ev2) | |
| NGC 1407 | NE | - | SR | | unusual shape |
| NGC 1549 | Lw | - | FR | | |
| NGC 1700 | Lw | cne? | FR | nD+G(Ev2) | |
| NGC 2974 | ??? | cne IC? | FR | Obsc AGN? | |
| NGC 3557 | Lb | cne | FR | Dust disk(GMOS) | |
| NGC 3585 | Lw | - | FR | nD+G(Ev2) | |
| NGC 3904 | NE | - | FR | nD+G(Ev2) | |
| NGC 3923 | NE | - | SR | | Stellar shells |
| NGC 3962 | Ln? | cne IC | SR | | |
| NGC 4105 | L | cne IC | FR | nD+G(Ev3) | |
| NGC 4696 | Lb | cne | SR | | Rdshftd peak H α /NII/SII |
| NGC 5018 | Lcn | IC? | FR | nD+G(Ev2) | |
| NGC 5044 | Lb | cne | FR? | | |
| NGC 6868 | Lb? | cne IC | SR | Obsc. AGN | |
| NGC 7507 | NE | - | SR | nD+G(Ev2) | |
| S0s | | | | | |
| NGC 1316 | L | cne IC | FR? | dust lane(HST) | |
| NGC 1332 | Ln? | cne? | FR | dust lane(GMOS?) | |
| NGC 1380 | Ln | cne | FR | dust disk (HST) nD+G(Ev2) | |
| NGC 1574 | L | cne IC? | FR | nD+G? | |
| NGC 2217 | S1.8 FC | cne IC | FR | | |
| NGC 2784 | Lwb? | | FR | | |
| NGC 3115 | *Lb | | FR | nD+G(Ev2) | Off-centered AGN |
| NGC 5101 | Ln | cne | FR | | |
| NGC 7049 | Lb | cne | FR | dust ring (HST) | |
| Spirals | | | | | |
| NGC 1300 | Lb? | cne | FR | nD+G(Ev2) | |
| NGC 4594 | Lb FC | cne | FR | nD+G?(Ev2) | M104 Sombr |
| NGC 4699 | Lb | cne | FR | | |

Notes: nD = nuclear dust +G=plus neutral gas; FR = Fast rotator; SR = Slow rotator; cne = circum-nuclear emission lines; IC= Ionization Cone; FC = featureless continuum; RG = Radio-galaxy; NE = no emission; L=LINER; Lw = weak LINER; Lb = LINER with broad H α ; *L=LINER detected only after subtracting the light from spectral synthesis.

Notes: Galaxies IC 1459, NGC 1052 and NGC 4594 (Sombrero) are Lb LINERs and NGC 2217 is a Sy galaxy with evidence of featureless continuum (FC), on the basis of the Fe I profile in Ev2.

The sub-sample of massive ($\sigma > 200$ km/s) galaxies

Preliminary statistics

With respect to the AGN

| | | |
|--------------------|----|------|
| Seyfert 1 galaxies | 1 | 3% |
| LINERs | 29 | 83% |
| No emission | 4 | 11% |
| ? | 1 | 3% |
| Total | 35 | 100% |

With respect to the LINER characteristics:

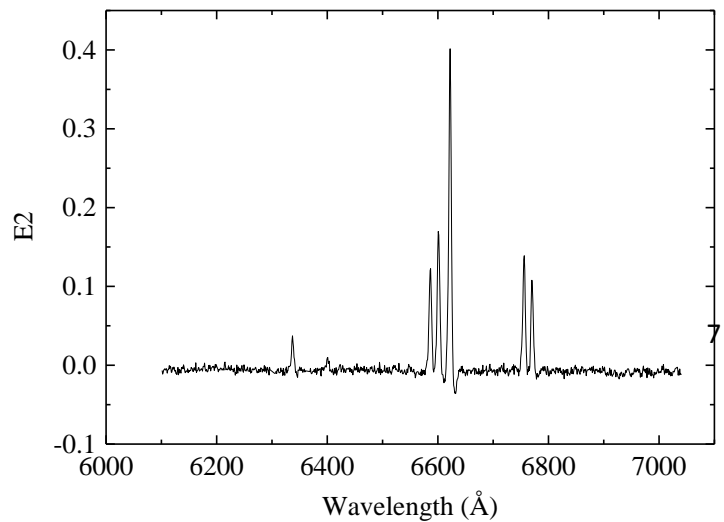
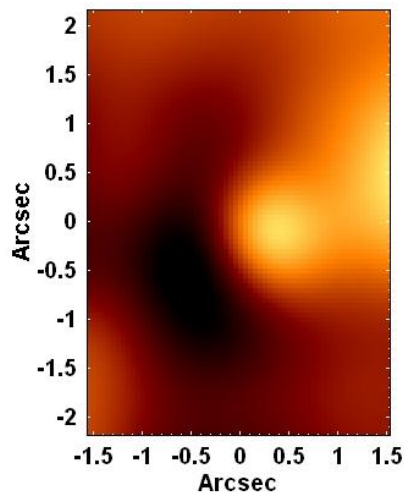
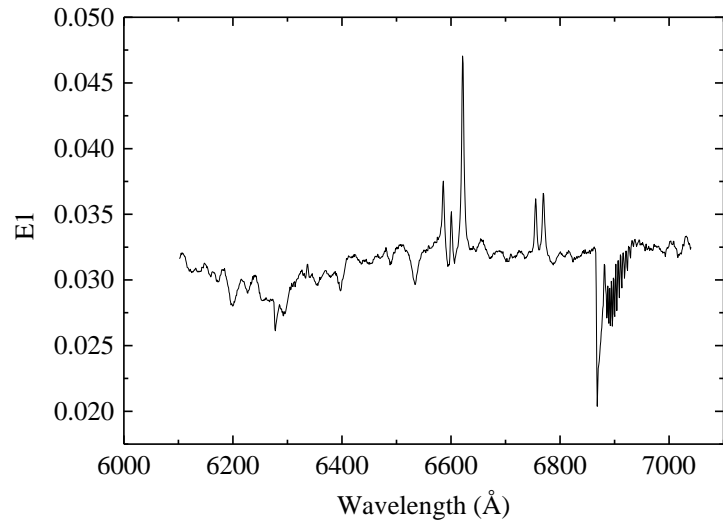
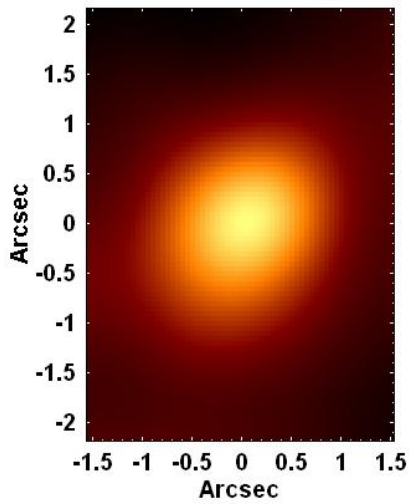
| | | |
|----|----|-----|
| Lb | 14 | 40% |
| Lw | 6 | 17% |
| L | 9 | 26% |

With respect to the extended characteristics:

| | | |
|-------------------------|----|-----|
| Circum-nuclear emission | 24 | 69% |
| Ionization cones | 9 | 26% |
| Fast rotators (stellar) | 24 | 69% |
| Slow rotators (stellar) | 11 | 31% |

Other properties:

| | | |
|-----------------------|----|-----|
| Dust present | 21 | 60% |
| Featureless Continuum | 4 | 11% |



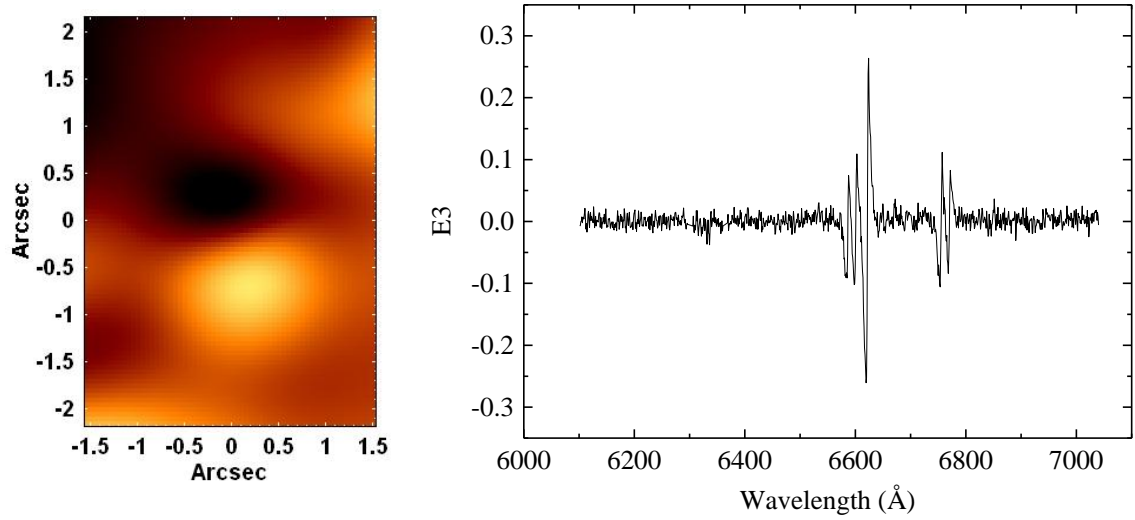


Figure 1 – PCA Tomography of NGC 1316 (For A). E1 represents the approximate contribution from the bulge+nucleus. E2 shows the ionization cone while E3 shows the disk of ionized gas. Notice that the disk and the cone are nearly perpendicular.

The Sc-Sd galaxy subsample

The observations of this sub-sample are still under way. We have already some observations in hand and we performed the analysis of three objects: NGC 300, NGC 1313 and NGC 7424.

The following steps were performed:

- 1- Wavelength and flux calibrations; DAR correction.
- 2- Fingerprint removal; spatial noise filtering (Buterworth filter); Richardson-Lucy deconvolution
- 3- Spectral synthesis (with Starlight software); stellar archeology.

We will only show two images of the results obtained for the galaxy NGC 7424. As can be seen in Figure 2, two main peaks of light are present, representing star formation events at 200 million and 500 million years ago. Old stellar populations (~ 10 billion years) are responsible for only about 10% of the total light of the center of this galaxy. In Fig 3 we show the maps of these populations as a function of metallicities. Diffuse emission at all metallicities is present.

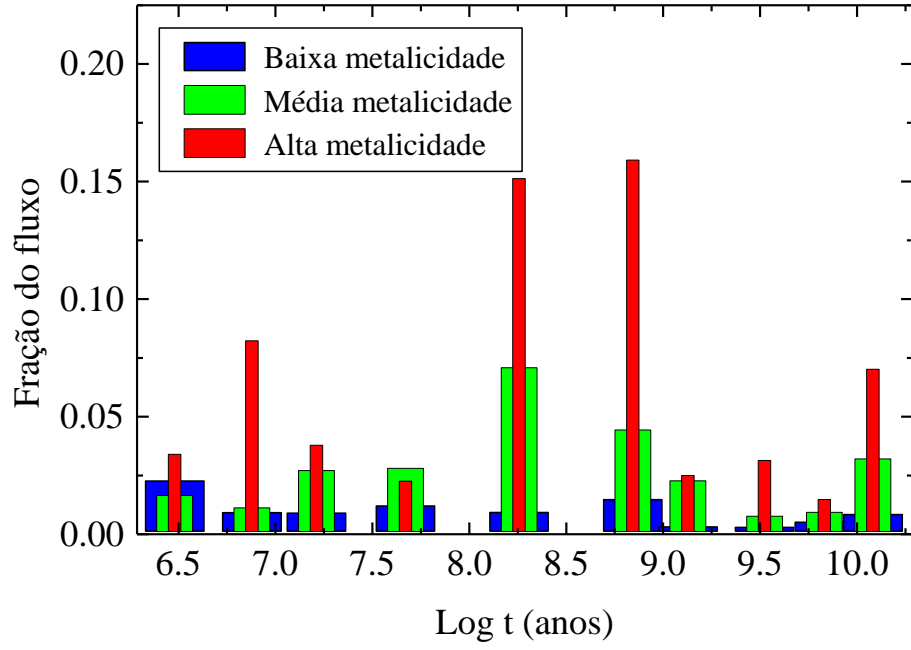


Figure 2 – Stellar archeology of the nucleus of the galaxy NGC 7424.

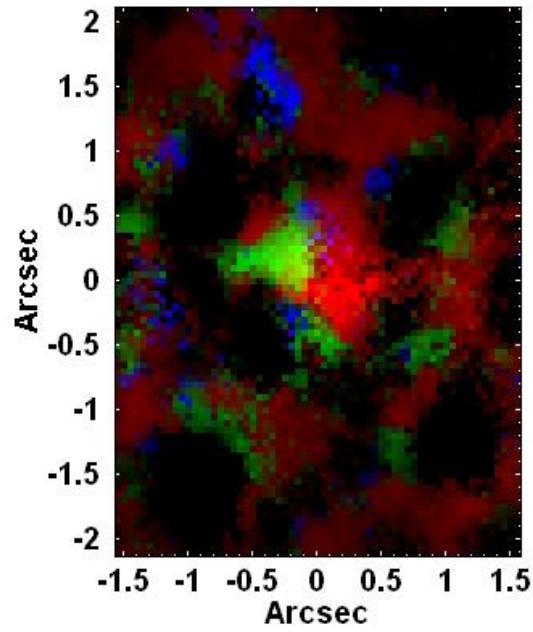


Figure 3 – The map of light emission of the population of 200 and 500 million years old. Red is high metallicity (0.02-0.05), green is medium metallicity (0.004-0.008) and blue, low metallicity (0.0001-0.0004).

Relevant publications:

A- Publications by our group involving objects from the DIVING^{3D} project, observed with the Gemini telescopes GMOS IFU:

Menezes, R. B. 2012 - PhD Thesis – Universidade de São Paulo

Ricci, T. V. 2013 - PhD Thesis -Universidade de São Paulo

Menezes, R. B., Steiner, J. E., Ricci, T. V. 2013 Ap J 765, L40

Ricci, T. V., Steiner, J. E. & Menezes, R. B. 2014a MNRAS, in press (see Astroph)

Ricci, T. V., Steiner, J. E. & Menezes, R. B. 2014b MNRAS, in press (see Astroph)

B- Publications involving observations with the Gemini telescopes IFUs that are related to the project in terms of methodology

Steiner, J. E., Menezes, R. B., Ricci, T. V. & Oliveira, A. S. 2009, MNRAS, 395, 64

Steiner, J. E., Menezes, R. B., Ricci, T. V. & Oliveira, A. S. 2009, MNRAS 396, 788

Ricci, T. V., Steiner, J. E. & Menezes, R. B. 2011, ApJ, 734, L10

Menezes, R. B., Steiner, J. E. & Ricci, T. V. 2013 Ap J 762, L29

Menezes, R. B., steiner, J. E. & Ricci, T. V. 2014, MNRAS 438, 2597

Appendix A – List of all galaxies in the project

| Num | Name | Type (NED) | RA J2000 | DE J2000 | B(T) | Activity | d (Mpc) |
|-----|---------|-------------------------------|--------------|--------------|-------|----------|---------|
| 1 | NGC 134 | SAB(s)bc | 00h30m21.97s | -33d14m38.5s | 10.96 | | 18.88 |
| 2 | NGC 150 | SB(rs)b? | 00h34m15.48s | -27d48m12.9s | 11.75 | | 21.04 |
| 3 | NGC 157 | SAB(rs)bc | 00h34m46.76s | -08d23m47.2s | 11.04 | | 19.5 |
| 4 | NGC 210 | SAB(s)b | 00h40m35.02s | -13d52m22.1s | 11.65 | | 20.98 |
| 5 | NGC 247 | SAB(s)d | 00h47m08.55s | -20d45m37.4s | 9.51 | | 3.59 |
| 6 | NGC 253 | SAB(s)c | 00h47m33.12s | -25d17m17.6s | 8.13 | | 3.14 |
| 7 | NGC 289 | SB(rs)bc | 00h52m42.36s | -31d12m21.0s | 11.81 | | 22.77 |
| 8 | NGC 300 | SA(s)d | 00h54m53.48s | -37d41m03.8s | 8.7 | | 1.97 |
| 9 | NGC 578 | SAB(rs)c | 01h30m29.09s | -22d40m02.5s | 11.48 | | 21.84 |
| 10 | NGC 584 | E4 | 01h31m20.75s | -06d52m05.0s | 11.2 | | 19.93 |
| 11 | NGC 596 | cD pec? | 01h32m52.08s | -07d01m54.6s | 11.88 | | 21.51 |
| 12 | NGC 613 | SB(rs)bc | 01h34m18.17s | -29d25m06.1s | 10.75 | Sy ? | 25.13 |
| 13 | NGC 685 | SAB(r)c | 01h47m42.81s | -52d45m42.5s | 11.97 | | 15.2 |
| 14 | NGC 720 | E5 | 01h53m00.50s | -13d44m19.2s | 11.15 | | 23.74 |
| 15 | NGC 779 | SAB(r)b | 01h59m42.28s | -05d57m47.5s | 11.86 | | 17.68 |
| 16 | NGC 908 | SA(s)c | 02h23m04.57s | -21d14m01.9s | 10.87 | | 17.62 |
| 17 | NGC 936 | SB0 ⁺ (rs) | 02h27m37.46s | -01d09m22.6s | 11.19 | | 20.68 |
| 18 | NGC 986 | SB(rs)ab | 02h33m34.35s | -39d02m42.2s | 11.8 | | 17.15 |
| 19 | NGC1042 | SAB(rs)cd | 02h40m23.97s | -08d26m00.8s | 11.49 | | 9.43 |
| 20 | NGC1052 | E4 | 02h41m04.80s | -08d15m20.8s | 11.53 | FSRS | 19.48 |
| 21 | NGC1068 | (R)SA(rs)b | 02h42m40.71s | -00d00m47.8s | 9.55 | Sy 2 | 13.5 |
| 22 | NGC1084 | SA(s)c | 02h45m59.91s | -07d34m42.5s | 11.25 | | 21.23 |
| 23 | NGC1097 | SB(s)b | 02h46m19.05s | -30d16m29.6s | 10.16 | LINER b | 20.04 |
| 24 | NGC1087 | SAB(rs)c | 02h46m25.16s | -00d29m55.1s | 11.56 | | 17.51 |
| 25 | NGC1187 | SB(r)c | 03h02m37.59s | -22d52m01.8s | 10.93 | | 18.83 |
| 26 | NGC1201 | SA0 ⁺ 0(r)? | 03h04m07.98s | -26d04m10.7s | 11.56 | | 20.37 |
| 27 | NGC1232 | SAB(rs)c | 03h09m45.51s | -20d34m45.5s | 10.5 | | 18.67 |
| 28 | NGC1249 | SB(s)cd | 03h10m01.23s | -53d20m08.7s | 11.8 | | 15.85 |
| 29 | NGC1255 | SAB(rs)bc | 03h13m32.04s | -25d43m30.6s | 11.6 | | 21.51 |
| 30 | NGC1291 | (R)SB0/a(s) | 03h17m18.59s | -41d06m29.0s | 9.42 | | 8.6 |
| 31 | NGC1313 | SB(s)d | 03h18m16.05s | -66d29m53.7s | 9.37 | | 3.95 |
| 32 | NGC1300 | SB(rs)bc | 03h19m41.08s | -19d24m40.9s | 11.1 | | 18.05 |
| 33 | NGC1302 | (R)SB0/a(r) | 03h19m51.18s | -26d03m37.6s | 11.38 | | 20 |
| 34 | NGC1316 | SAB0 ⁺ 0(s) pec | 03h22m41.72s | -37d12m29.6s | 9.6 | | 19.99 |
| 35 | NGC1326 | (R)SB0 ⁺ +(r) | 03h23m56.40s | -36d27m52.8s | 11.34 | | 16.98 |
| 36 | NGC1332 | S0 ⁺ -?(s) edge-on | 03h26m17.25s | -21d20m06.8s | 11.29 | | 19.62 |
| 37 | NGC1344 | E5 | 03h28m19.67s | -31d04m05.4s | 11.28 | | 18.69 |
| 38 | NGC1350 | (R')SB(r)ab | 03h31m08.12s | -33d37m43.1s | 11.4 | | 20.94 |
| 39 | NGC1365 | SB(s)b | 03h33m36.37s | -36d08m25.4s | 10.21 | Sy 1.8 | 17.93 |
| 40 | NGC1371 | SAB(rs)a | 03h35m01.34s | -24d55m59.6s | 11.5 | | 23.25 |
| 41 | NGC1380 | SA0 | 03h36m27.59s | -34d58m34.4s | 11.1 | | 18.55 |
| 42 | NGC1387 | SAB0 ⁺ -(s) | 03h36m57.06s | -35d30m23.9s | 11.83 | | 17.24 |
| 43 | NGC1385 | SB(s)cd | 03h37m28.85s | -24d30m01.1s | 11.65 | | 14.95 |

| | | | | | | | |
|----|---------|---------------------------|--------------|--------------|-------|--------|-------|
| 44 | NGC1395 | E2 | 03h38m29.75s | -23d01m39.1s | 11.18 | | 21.52 |
| 45 | NGC1399 | E1 pec | 03h38m29.03s | -35d27m02.4s | 10.79 | Sy 2 | 17.92 |
| 46 | NGC1411 | SA0 ⁺ -(r)? | 03h38m44.87s | -44d06m02.2s | 11.7 | | 15.5 |
| 47 | NGC1404 | E1 | 03h38m51.92s | -35d35m39.8s | 11.06 | | 18.72 |
| 48 | NGC1398 | (R')SB(r)ab | 03h38m52.13s | -26d20m16.2s | 10.6 | | 21.03 |
| 49 | NGC1407 | E0 | 03h40m11.86s | -18d34m48.4s | 10.93 | | 23.11 |
| 50 | NGC1433 | (R')SB(r)ab | 03h42m01.55s | -47d13m19.5s | 10.68 | | 9.96 |
| 51 | NGC1425 | SA(s)b | 03h42m11.47s | -29d53m36.0s | 11.6 | | 21.26 |
| 52 | NGC1427 | cD | 03h42m19.42s | -35d23m33.2s | 11.94 | | 19.36 |
| 53 | NGC1421 | SAB(rs)bc? | 03h42m29.28s | -13d29m16.9s | 11.95 | | 26.38 |
| 54 | NGC1448 | SAcd? edge-on | 03h44m31.92s | -44d38m41.4s | 11.3 | | 17.45 |
| 55 | NGC1493 | SB(r)cd | 03h57m27.43s | -46d12m38.5s | 11.82 | | 11.3 |
| 56 | NGC1512 | SB(r)a | 04h03m54.28s | -43d20m55.9s | 11.38 | | 12.29 |
| 57 | NGC1515 | SAB(s)bc | 04h04m02.72s | -54d06m00.2s | 11.93 | | 16.86 |
| 58 | NGC1527 | SAB0 ⁺ -(r)? | 04h08m24.14s | -47d53m49.3s | 11.7 | | 16.62 |
| 59 | NGC1533 | SB0 ⁺ - | 04h09m51.84s | -56d07m06.4s | 11.71 | | 18.38 |
| 60 | NGC1532 | SB(s)b pec ed-on | 04h12m04.33s | -32d52m27.2s | 11.53 | | 17.05 |
| 61 | NGC1543 | (R)SB0 ⁺ 0(s) | 04h12m43.25s | -57d44m16.7s | 11.49 | | 17.2 |
| 62 | NGC1537 | SAB0 ⁺ - pec? | 04h13m40.71s | -31d38m43.5s | 11.62 | | 18.48 |
| 63 | NGC1549 | E0-1 | 04h15m45.13s | -55d35m32.1s | 10.76 | | 16.33 |
| 64 | NGC1553 | SA0 ⁺ 0(r) | 04h16m10.47s | -55d46m48.5s | 10.42 | | 15.08 |
| 65 | NGC1559 | SB(s)cd | 04h17m35.77s | -62d47m01.2s | 10.97 | | 15.68 |
| 66 | NGC1566 | SAB(s)bc | 04h20m00.42s | -54d56m16.1s | 10.21 | Sy 1.5 | 12.23 |
| 67 | NGC1574 | SA0 ⁺ -(s)? | 04h21m58.82s | -56d58m29.1s | 11.19 | | 18.65 |
| 68 | NGC1617 | SB(s)a | 04h31m39.53s | -54d36m08.2s | 11.37 | | 13.4 |
| 69 | NGC1637 | SAB(rs)c | 04h41m28.18s | -02d51m28.7s | 11.52 | | 10.7 |
| 70 | NGC1672 | SB(s)b | 04h45m42.50s | -59d14m49.9s | 11.03 | Sy | 14.5 |
| 71 | NGC1700 | E4 | 04h56m56.31s | -04d51m56.8s | 11.96 | | 41.08 |
| 72 | NGC1744 | SB(s)d | 04h59m57.80s | -26d01m20.0s | 11.7 | | 10.85 |
| 73 | NGC1792 | SA(rs)bc | 05h05m14.45s | -37d58m50.7s | 10.85 | | 13.2 |
| 74 | NGC1808 | (R)SAB(s)a | 05h07m42.34s | -37d30m47.0s | 10.7 | H II | 11.55 |
| 75 | NGC1947 | S0 ⁺ - pec | 05h26m47.61s | -63d45m36.1s | 11.86 | | 16.3 |
| 76 | NGC1964 | SAB(s)b | 05h33m21.76s | -21d56m44.8s | 11.6 | | 21.41 |
| 77 | NGC2090 | SA(rs)c | 05h47m01.89s | -34d15m02.2s | 11.85 | | 12.76 |
| 78 | NGC2207 | SAB(rs)bc pec | 06h16m22.03s | -21d22m21.6s | 11.35 | | 26.5 |
| 79 | NGC2217 | (R)SB0 ⁺ +(rs) | 06h21m39.78s | -27d14m01.5s | 11.59 | | 19.5 |
| 80 | NGC2442 | SAB(s)bc pec | 07h36m23.84s | -69d31m51.0s | 11.16 | LINER | 17.1 |
| 81 | NGC2784 | SA0 ⁺ 0(s)? | 09h12m19.50s | -24d10m21.4s | 11.21 | | 8.45 |
| 82 | NGC2835 | SB(rs)c | 09h17m52.91s | -22d21m16.8s | 10.95 | | 10.82 |
| 83 | NGC2974 | E4 | 09h42m33.28s | -03d41m56.9s | 11.78 | Sy 2 | 24.73 |
| 84 | NGC2997 | SAB(rs)c | 09h45m38.79s | -31d11m27.9s | 10.32 | FSRS | 10.77 |
| 85 | NGC3115 | S0 ⁺ - edge-on | 10h05m13.98s | -07d43m06.9s | 9.98 | | 10.17 |
| 86 | NGC3223 | SA(s)b | 10h21m35.08s | -34d16m00.5s | 11.88 | | 33.37 |
| 87 | NGC3511 | SA(s)c | 11h03m23.77s | -23d05m12.4s | 11.56 | | 14.28 |
| 88 | NGC3513 | SB(rs)c | 11h03m46.08s | -23d14m43.8s | 11.99 | | 13.15 |

| | | | | | | | |
|-----|---------|----------------------------|--------------|--------------|-------|----------|-------|
| 89 | NGC3557 | E3 | 11h09m57.64s | -37d32m21.0s | 11.46 | FSRS | 36.18 |
| 90 | NGC3585 | E6 | 11h13m17.09s | -26d45m17.4s | 10.93 | | 18.21 |
| 91 | NGC3621 | SA(s)d | 11h18m16.51s | -32d48m50.6s | 10.03 | | 6.76 |
| 92 | NGC3672 | SA(s)c | 11h25m02.47s | -09d47m43.4s | 11.66 | | 27.12 |
| 93 | NGC3887 | SB(r)bc | 11h47m04.57s | -16d51m16.6s | 11.6 | | 19.3 |
| 94 | NGC3904 | E2-3? | 11h49m13.22s | -29d16m36.3s | 11.95 | | 24.66 |
| 95 | NGC3923 | E4-5 | 11h51m01.69s | -28d48m21.7s | 10.91 | | 20.88 |
| 96 | NGC3962 | E1 | 11h54m40.10s | -13d58m30.1s | 11.66 | | 30.73 |
| 97 | NGC4030 | SA(s)bc | 12h00m23.63s | -01d06m00.3s | 11.07 | | 24.46 |
| 98 | NGC4105 | E3 | 12h06m40.77s | -29d45m36.8s | 11.88 | | 27.7 |
| 99 | NGC4487 | SAB(rs)cd | 12h31m04.46s | -08d03m14.1s | 11.66 | | 20.04 |
| 100 | NGC4504 | SA(s)cd | 12h32m17.45s | -07d33m48.4s | 11.92 | | 21.81 |
| 101 | NGC4546 | SB0 ⁺ -(s)? | 12h35m29.51s | -03d47m35.5s | 11.3 | | 18.1 |
| 102 | NGC4593 | (R)SB(rs)b | 12h39m39.43s | -05d20m39.3s | 11.72 | Sy | 33.93 |
| 103 | NGC4594 | SA(s)a edge-on | 12h39m59.43s | -11d37m23.0s | 9.28 | Unb Sy 2 | 10.39 |
| 104 | NGC4666 | SABc? | 12h45m08.59s | -00d27m42.8s | 11.56 | | 18.22 |
| 105 | NGC4691 | (R)SB0/a(s) pec | 12h48m13.63s | -03d19m57.8s | 11.7 | | 22.5 |
| 106 | NGC4697 | E6 | 12h48m35.88s | -05d48m02.7s | 10.11 | | 12.31 |
| 107 | NGC4696 | cD1 pec | 12h48m49.25s | -41d18m39.0s | 11.59 | LINER | 38.04 |
| 108 | NGC4699 | SAB(rs)b | 12h49m02.23s | -08d39m53.5s | 10.44 | | 24.7 |
| 109 | NGC4731 | SB(s)cd | 12h51m01.09s | -06d23m35.0s | 11.55 | | 19.75 |
| 110 | NGC4753 | I0 | 12h52m22.11s | -01d11m58.9s | 10.85 | | 16.87 |
| 111 | NGC4775 | SA(s)d | 12h53m45.70s | -06d37m19.8s | 11.74 | | 26.6 |
| 112 | NGC4781 | SB(rs)d | 12h54m23.75s | -10d32m13.9s | 11.69 | | 16.12 |
| 113 | NGC4818 | SAB(rs)ab pec? | 12h56m48.90s | -08d31m31.1s | 11.89 | | 20.05 |
| 114 | NGC4856 | SB0/a(s) | 12h59m21.27s | -15d02m31.8s | 11.4 | | 21.1 |
| 115 | NGC4902 | SB(r)b | 13h00m59.73s | -14d30m49.1s | 11.9 | | 39.2 |
| 116 | NGC4941 | (R)SAB(r)ab? | 13h04m13.14s | -05d33m05.8s | 11.9 | Sy 2 | 18.22 |
| 117 | NGC4939 | SA(s)bc | 13h04m14.39s | -10d20m22.6s | 11.56 | Sy 2 | 38.99 |
| 118 | NGC4958 | SB0(r)? edge-on | 13h05m48.88s | -08d01m13.0s | 11.48 | | 18.47 |
| 119 | NGC4981 | SAB(r)bc | 13h08m48.74s | -06d46m39.1s | 11.83 | | 24.72 |
| 120 | NGC4984 | (R)SAB0 ⁺ +(rs) | 13h08m57.23s | -15d30m58.7s | 11.71 | | 21.3 |
| 121 | NGC4995 | SAB(rs)b | 13h09m40.65s | -07d50m00.3s | 11.9 | | 28.91 |
| 122 | NGC5018 | E3? | 13h13m01.03s | -19d31m05.5s | 11.71 | | 37.66 |
| 123 | NGC5044 | E0 | 13h15m23.97s | -16d23m07.9s | 11.92 | | 35 |
| 124 | NGC5054 | SA(s)bc | 13h16m58.49s | -16d38m05.5s | 11.51 | | 19.85 |
| 125 | NGC5061 | E0 | 13h18m05.07s | -26d50m14.0s | 11.35 | | 25.58 |
| 126 | NGC5068 | SAB(rs)cd | 13h18m54.81s | -21d02m20.8s | 10.53 | | 6.07 |
| 127 | NGC5101 | (R)SB0/a(rs) | 13h21m46.24s | -27d25m49.9s | 11.58 | | 27.4 |
| 128 | NGC5102 | SA0 ⁺ - | 13h21m57.61s | -36d37m48.9s | 10.64 | | 18.78 |
| 129 | NGC5128 | S0 pec | 13h25m27.62s | -43d01m08.8s | 7.89 | | 3.66 |
| 130 | NGC5161 | SA(s)c? | 13h29m13.91s | -33d10m25.8s | 11.98 | | 24.27 |
| 131 | NGC5170 | SA(s)c? ed-on | 13h29m48.79s | -17d57m59.1s | 11.88 | | 27.29 |
| 132 | IC 4296 | E | 13h36m39.03s | -33d57m57.0s | 11.58 | FSRS | 50.21 |
| 133 | NGC5236 | SAB(s)c | 13h37m00.95s | -29d51m55.5s | 8.51 | FSRS | 6.96 |

| | | | | | | | |
|-----|---------|--------------------------|--------------|--------------|-------|--------|-------|
| 134 | NGC5247 | SA(s)bc | 13h38m03.04s | -17d53m02.5s | 11.1 | | 22.2 |
| 135 | NGC5334 | SB(rs)c? | 13h52m54.46s | -01d06m52.7s | 11.9 | | 32.62 |
| 136 | NGC5530 | SA(rs)bc | 14h18m27.15s | -43d23m18.9s | 11.98 | | 14.3 |
| 137 | NGC5556 | SAB(rs)d | 14h20m34.09s | -29d14m30.4s | 11.88 | | 18.75 |
| 138 | NGC5584 | SAB(rs)cd | 14h22m23.77s | -00d23m15.6s | 11.95 | | 26.74 |
| 139 | NGC5643 | SAB(rs)c | 14h32m40.74s | -44d10m27.9s | 10.89 | Sy 2 | 16.9 |
| 140 | NGC5792 | SB(rs)b | 14h58m22.71s | -01d05m27.9s | 11.72 | | 24.44 |
| 141 | NGC6118 | SA(s)cd | 16h21m48.62s | -02d17m00.4s | 11.91 | | 23.37 |
| 142 | NGC6684 | (R')SB0 ⁰ (s) | 18h48m57.88s | -65d10m24.4s | 11.34 | | 12.44 |
| 143 | NGC6744 | SAB(r)bc | 19h09m46.10s | -63d51m27.1s | 9.24 | | 9.5 |
| 144 | NGC6753 | (R)SA(r)b | 19h11m23.64s | -57d02m58.4s | 11.93 | | |
| 145 | NGC6868 | E2 | 20h09m54.07s | -48d22m46.4s | 11.83 | FSRS | 31.58 |
| 146 | NGC7049 | SA0 ⁰ (s) | 21h19m00.30s | -48d33m43.8s | 11.64 | | 28.2 |
| 147 | NGC7083 | SA(s)bc | 21h35m44.69s | -63d54m10.2s | 11.8 | | 33.26 |
| 148 | NGC7090 | SBc? edge-on | 21h36m28.86s | -54d33m26.4s | 11.1 | | 8.4 |
| 149 | NGC7144 | E0 | 21h52m42.43s | -48d15m13.5s | 11.79 | | 25.46 |
| 150 | NGC7184 | SB(r)c | 22h02m39.82s | -20d48m46.2s | 11.67 | | 33.6 |
| 151 | NGC7205 | SA(s)bc | 22h08m34.29s | -57d26m33.3s | 11.57 | | 19.39 |
| 152 | NGC7213 | SA(s)a? | 22h09m16.31s | -47d09m59.8s | 11.18 | FSRS | 22 |
| 153 | IC 5201 | SB(rs)cd | 22h20m57.44s | -46d02m09.1s | 11.54 | | 14.4 |
| 154 | NGC7314 | SAB(rs)bc | 22h35m46.19s | -26d03m01.7s | 11.65 | Sy 1 h | 18.5 |
| 155 | NGC7410 | SB(s)a | 22h55m00.95s | -39d39m40.8s | 11.3 | LINER | 20.1 |
| 156 | IC 1459 | E3-4 | 22h57m10.61s | -36d27m44.0s | 10.96 | FSRS | 26.99 |
| 157 | IC 5267 | SA0/a(s) | 22h57m13.57s | -43d23m46.1s | 11.39 | | 26.08 |
| 158 | NGC7424 | SAB(rs)cd | 22h57m18.37s | -41d04m14.1s | 10.99 | | 11.5 |
| 159 | IC 5273 | SB(rs)cd? | 22h59m26.70s | -37d42m10.4s | 11.9 | | 16.56 |
| 160 | NGC7496 | SB(s)b | 23h09m47.29s | -43d25m40.6s | 11.78 | Sy 2 | 15.02 |
| 161 | NGC7507 | E0 | 23h12m07.59s | -28d32m22.6s | 11.43 | | 22.5 |
| 162 | NGC7552 | (R')SB(s)ab | 23h16m10.76s | -42d35m05.1s | 11.4 | H II | 17.15 |
| 163 | NGC7582 | (R')SB(s)ab | 23h18m23.50s | -42d22m14.0s | 11.46 | Sy 1 i | 20.62 |
| 164 | NGC7606 | SA(s)b | 23h19m04.78s | -08d29m06.3s | 11.55 | | 31.55 |
| 165 | IC 5328 | E4 | 23h33m16.46s | -45d00m57.5s | 11.95 | | 34.74 |
| 166 | IC 5332 | SA(s)d | 23h34m27.49s | -36d06m03.9s | 11.25 | | 8.4 |
| 167 | NGC7713 | SB(r)d? | 23h36m14.99s | -37d56m17.1s | 11.65 | | 10.27 |
| 168 | NGC7723 | SB(r)b | 23h38m57.08s | -12d57m39.9s | 11.85 | | 27.37 |
| 169 | NGC7727 | SAB(s)a pec | 23h39m53.72s | -12d17m34.0s | 11.55 | | 23.3 |
| 170 | NGC7793 | SA(s)d | 23h57m49.83s | -32d35m27.7s | 9.65 | | 4.17 |

List of galaxies that are not part of the survey. These galaxies do not have a nucleus that can be identified in order to point the telescope. They are typically classified as Sm.

| Num | Name | Type (NED) | _RAJ2000 | _DEJ2000 | B(T) | Activity | d (Mpc) |
|-----|--------|---------------|--------------|--------------|------|----------|---------|
| 1 | LMC | SB(s)m | 05h23m34.53s | -69d45m22.1s | 0.63 | | 0.05 |
| 2 | SMC | SB(s)m pec | 00h52m44.78s | -72d49m43.0s | 2.79 | | 0.06 |
| 3 | NGC 55 | SB(s)m? ed-on | 00h14m53.60s | -39d11m47.9s | 8.22 | | 1.94 |

| | | | | | | |
|----|----------|--------------|--------------|--------------|-------|-----------|
| 4 | A0237-34 | dE4 | 02h39m59.3s | -34d26m57s | 9.04 | 0.14 |
| 5 | NGC6822 | IB(s)m | 19h44m57.74s | -14d48m12.4s | 9.35 | 0.5 |
| 6 | NGC3109 | SB(s)m ed-on | 10h03m06.88s | -26d09m34.5s | 10.39 | 1.32 |
| 7 | NGC 45 | SA(s)dm | 00h14m03.99s | -23d10m55.5s | 11.1 | 9.31 |
| 8 | NGC5253 | pec | 13h39m55.96s | -31d38m24.4s | 11.11 | FSRS 3.67 |
| 9 | NGC4038 | SB(s)m pec | 12h01m53.01s | -18d52m03.4s | 11.3 | 20.88 |
| 10 | A2359-15 | IB(s)m | 00h01m58.1s | -15d27m39s | 11.4 | 1.11 |
| 11 | NGC4027 | SB(s)dm | 11h59m30.17s | -19d15m54.8s | 11.65 | 25.6 |
| 12 | IC 5152 | IA(s)m | 22h02m41.51s | -51d17m47.2s | 11.68 | 1.76 |
| 13 | IC 4662 | IBm | 17h47m08.87s | -64d38m30.3s | 11.76 | 2.44 |
| 14 | A1008-04 | IBm | 10h11m00.8s | -04d41m34s | 11.87 | 1.44 |

Appendix B – Galaxies with known nuclear activity, according to NED.

| Num | Name | Type (NED) | RAJ2000 | DEJ2000 | B(T) | Activity | d (Mpc) |
|-----|---------|----------------|--------------|--------------|-------|----------|---------|
| 1 | NGC 613 | SB(rs)bc | 01h34m18.17s | -29d25m06.1s | 10.75 | Sy ? | 25.13 |
| 2 | NGC1052 | E4 | 02h41m04.80s | -08d15m20.8s | 11.53 | FSRS | 19.48 |
| 3 | NGC1068 | (R)SA(rs)b | 02h42m40.71s | -00d00m47.8s | 9.55 | Sy 2 | 13.5 |
| 4 | NGC1097 | SB(s)b | 02h46m19.05s | -30d16m29.6s | 10.16 | LINER b | 20.04 |
| 5 | NGC1365 | SB(s)b | 03h33m36.37s | -36d08m25.4s | 10.21 | Sy 1.8 | 17.93 |
| 6 | NGC1399 | E1 pec | 03h38m29.03s | -35d27m02.4s | 10.79 | Sy 2 | 17.92 |
| 7 | NGC1566 | SAB(s)bc | 04h20m00.42s | -54d56m16.1s | 10.21 | Sy 1.5 | 12.23 |
| 8 | NGC1672 | SB(s)b | 04h45m42.50s | -59d14m49.9s | 11.03 | Sy | 14.5 |
| 9 | NGC1808 | (R)SAB(s)a | 05h07m42.34s | -37d30m47.0s | 10.7 | H II | 11.55 |
| 10 | NGC2442 | SAB(s)bc pec | 07h36m23.84s | -69d31m51.0s | 11.16 | LINER | 17.1 |
| 11 | NGC2974 | E4 | 09h42m33.28s | -03d41m56.9s | 11.78 | Sy 2 | 24.73 |
| 12 | NGC2997 | SAB(rs)c | 09h45m38.79s | -31d11m27.9s | 10.32 | FSRS | 10.77 |
| 13 | NGC3557 | E3 | 11h09m57.64s | -37d32m21.0s | 11.46 | FSRS | 36.18 |
| 14 | NGC4593 | (R)SB(rs)b | 12h39m39.43s | -05d20m39.3s | 11.72 | Sy | 33.93 |
| 15 | NGC4594 | SA(s)a edge-on | 12h39m59.43s | -11d37m23.0s | 9.28 | Unb Sy 2 | 10.39 |
| 16 | NGC4696 | cD1 pec | 12h48m49.25s | -41d18m39.0s | 11.59 | LINER | 38.04 |
| 17 | NGC4941 | (R)SAB(r)ab? | 13h04m13.14s | -05d33m05.8s | 11.9 | Sy 2 | 18.22 |
| 18 | NGC4939 | SA(s)bc | 13h04m14.39s | -10d20m22.6s | 11.56 | Sy 2 | 38.99 |
| 19 | IC 4296 | E | 13h36m39.03s | -33d57m57.0s | 11.58 | FSRS | 50.21 |
| 20 | NGC5236 | SAB(s)c | 13h37m00.95s | -29d51m55.5s | 8.51 | FSRS | 6.96 |
| 21 | NGC5643 | SAB(rs)c | 14h32m40.74s | -44d10m27.9s | 10.89 | Sy 2 | 16.9 |
| 22 | NGC6868 | E2 | 20h09m54.07s | -48d22m46.4s | 11.83 | FSRS | 31.58 |
| 23 | NGC7213 | SA(s)a? | 22h09m16.31s | -47d09m59.8s | 11.18 | FSRS | 22 |
| 24 | NGC7314 | SAB(rs)bc | 22h35m46.19s | -26d03m01.7s | 11.65 | Sy 1 h | 18.5 |
| 25 | NGC7410 | SB(s)a | 22h55m00.95s | -39d39m40.8s | 11.3 | LINER | 20.1 |
| 26 | IC 1459 | E3-4 | 22h57m10.61s | -36d27m44.0s | 10.96 | FSRS | 26.99 |
| 27 | NGC7496 | SB(s)b | 23h09m47.29s | -43d25m40.6s | 11.78 | Sy 2 | 15.02 |
| 28 | NGC7552 | (R')SB(s)ab | 23h16m10.76s | -42d35m05.1s | 11.4 | H II | 17.15 |
| 29 | NGC7582 | (R')SB(s)ab | 23h18m23.50s | -42d22m14.0s | 11.46 | Sy 1 i | 20.62 |
| | Name | Type (NED) | _RAJ2000 | _DEJ2000 | B(T) | Activity | d (Mpc) |
| 1 | NGC5253 | pec | 13h39m55.96s | -31d38m24.4s | 11.11 | FSRS | 3.67 |

Appendix C: The original proposal

Abstract

Galactic nuclei are special regions of galaxies, hosting supermassive black holes and stellar populations that record important aspects of the history of the galaxy formation and evolution. In this proposal we aim to perform a survey of nuclei of a complete sample with deep 3D spectroscopy, with a combination of unprecedented spatial resolution and signal-to noise.

We expect to achieve 4 scientific goals: a-***Nuclear emission line properties***. Detect and study the statistical, geometric and physical properties of Low Luminosity AGN: “dwarf” Seyferts and LINERs as well as starburst nuclei. We propose to carry out the deepest demographic study of supermassive black holes and their local environment yet performed. b-***Circum-nuclear emission line properties***. Determine the nature and ionization mechanism as well as the kinematics of the line emitting gas in the ~ 100 pc scale circum-nuclear region. c-***Stellar kinematical properties*** of all nuclei. Mass-to-light ratios will be derived on dynamical basis and compared to those of spectral synthesis and stellar velocity dispersion in order to study the importance of dark matter and the IMF. d-***Stellar populations archeology***. Study the chemical composition and history of star formation using state-of the-art methods and stellar population models.

The Science Case

Galaxies have been known as entities containing hundreds of billions of stars - islands in the universe - for about 90 years. Their nuclei certainly preserve important information about their origin and evolution. For these reasons it is important to study them, both at the individual level and on a statistical basis. Besides the stellar emission, many galactic nuclei present emission lines that are not originated by stars. They are frequently called Active Galactic Nuclei (AGNs). The luminosity function of AGN is such that they can be studied at large distances. Curiously the most abundant objects are of low luminosity (LLAGN) and not so well studied although abundantly populating the galaxies in the local universe. The LLAGN (as all AGNs) can be classified as type 1 (with broad permitted emission lines) or type 2, without broad emission lines. The presence of a broad component is considered a conclusive proof that the object contains a supermassive black hole.

Most of the massive galaxies host an active nucleus [1], the majority of them presenting low ionization emission lines and hence classified as LINERs (Low Ionization Nuclear Emission Regions [2]). The nuclear emission in LINERs has been proposed to be similar to that of Seyfert galaxies, but in an environment with lower ionization parameter [3, 4]; this idea was confirmed by the discovery of broad H α emission in a significant fraction of the LINERs as well as the detection of optical non-thermal continuum, high ionization forbidden lines and in X-Rays. Such characteristics are usually associated with a black hole. But it was also found that this low ionization emission can be quite extended in early type galaxies [5], far beyond the ionization produced by a low luminosity central source. The source of this ionization was proposed to be a population of post-AGB stars [6]. In the last two decades significant evidence of nuclear activity has been detected in LINER galaxies [1] but also the evidence of extended post-AGB ionized emission has grown [7-10]. Approximately two thirds of E-Sb galaxies exhibit local weak nuclear activity incompatible with normal stellar processes; in contrast, only about 15% of the Sc-Sm galaxies are known to have AGN activity [1]. Late type galaxies are generally of low mass, gas rich, with strong star formation, bulgeless or associated with pseudo-bulges. These galaxies are frequently characterized as having a central cluster [11, 12]. The nature of these clusters is still poorly understood and they are even considered as failed black holes [13]. It is now well accepted that AGN, Seyfert galaxies as well as most LINERs, are associated with supermassive black holes (BH), with masses ranging from 10^6 - $10^{10} M_{\odot}$. It

is also well established that there is a strong correlation between BH mass and host galaxy properties [14-16], which has generated great interest in studying the connections between BH growth and galaxy formation/evolution. As a direct manifestation of accretion and growth, BHs have been considered as essential components of structure formation [17-19]. An effective way of studying galaxies and their nuclei is by performing surveys of large samples. With such surveys, new and interesting objects have been found and, if the samples are selected by rigorous criteria, statistical properties can be derived. In this proposal we aim to study a complete sample of galaxies in the southern hemisphere with high (unprecedented) spatial resolution and high signal/noise.

Previous surveys of galaxies and their nuclei in the local universe have been done in the past and that are relevant to the present proposal. PALOMAR: The most popular survey of galactic nuclei [1, 20]. This work has generated a significant number of papers (see [1, 35] for recent reviews) with a large number of citations. This survey is based on single spectra taken with a 2"x4" slit on the Palomar 5 m telescope taken for every galaxy brighter than $B=12.5$ in the Revised Shapley-Ames Catalog of Bright Galaxies. A total of 486 galaxies satisfy this criterion in the northern hemisphere ($\delta > 0$). Important and influential as it was (and still is), the Palomar Survey offers no information on the spatial distribution of the light emitting/absorbing sources. That requires Integral Field Units (IFUs). With the coming of age of IFUs, survey studies are bringing additional capabilities of better studying not only the nucleus itself but also its environment. Some relevant IFU-based surveys are: SAURON – A sample of 327 galaxies were observed with the 4.2 m Herschel telescope [21]. In the low resolution mode the pixel size was $0.94'' \times 0.94''$ with a spectral resolution of 3.6 Å. The spectral coverage did not include the $H\alpha + [N II]$ as well as the $[O I]$ and $[S II]$ lines, very important to study the AGN. The sample included galaxies with $M_b < -18$ and $-6^\circ < \delta < 64^\circ$. ATLAS 3D - This survey [22] is an extension of SAURON, but for early type galaxies only. It, again, does not include the spectral coverage of important emission lines. CALIFA - This survey uses the 3.5 m telescope of Calar Alto to observe ~600 galaxies [23]. The main goal is to observe the whole galaxy in the FOV. For this reason the spatial resolution was degraded to $\sim 3''$ and is not optimized to study the nucleus. Other surveys such as MANGA and SAMI are being planned with IFUs to observe large samples at higher redshifts *a la* Sloan Survey.

The GSGN will obviously benefit from both the scientific insight and the analysis tools developed for these previous and ongoing IFU surveys. Yet, it will explore a spatial scale **not resolved** by these surveys. While CALIFA (as SAURON and ATLAS 3D) reveals the spatial arrangement of phenomena which are all mixed up in Palomar and SDSS data, GSGN will map physics which is blurred in the data cubes of those surveys. For instance, the GSGN FoV spans just ~ a couple of spatial resolution elements of CALIFA! GSGN will thus map physical processes in the nuclear and circum-nuclear scales (100 pc) to a degree of detail (20 pc resolution) which is completely **out of reach of other surveys**. No other IFU survey is aiming at this sweet spot region of galaxies, where high stellar and gaseous densities, high metallicities, presence of (active or dormant) supermassive black holes and other extreme conditions drive a variety phenomena seen nowhere else in galaxies: scattering cones, obscuring torus, the NLR, BLR, inflows and outflows, nuclear clusters, inner gaseous and stellar disks, etc.

The exquisite spatial resolution of GSGN will allow us to investigate the connection between AGN and its surrounding stellar population to an unprecedented level of spatial detail, shedding new light on long standing puzzles. For instance, while type 2 Seyferts show a clear tendency to host recent star-formation [38-41], it is unclear whether this also happens in type 1 Seyferts. The unadorned unified model implies that type 1s should also exhibit such young stars, but it may also be that, over time, the mechanical and radiative action of star formation and the AGN dissipates the obscuring torus, clearing the view towards the nucleus and making a type 2 evolve to a type 1. Studying this issue requires disentangling the different spectral components, which is best achieved through IFU of the inner ~ 100 pc.

The statistics of LLAGN is limited by the sensitivity of the detection techniques. We believe that, with the techniques developed by our group (30, 32, 36, 37, 50-52; see Figs 1 and 2), we are able to detect AGN at significant lower luminosity limits than the current level of

detection such as in the Palomar Survey. We base this belief on two facts: We are concluding a mini-survey of massive galactic nuclei, comprising an unbiased sample of 36 southern galaxies. Our preliminary statistics indicate that we found two times more objects with broad H α than anticipated from the Palomar survey. This is probably due to the fact that we have much better spatial resolution. A second and perhaps more important argument comes from the Log N x Log S analysis of AGN present in Sc-Sd galaxies. There is a very strong tendency of such objects to appear in the nearest galaxies only. In X-rays a larger proportion than expected has been detected but X-rays are poised by binaries and the statistics are not all that reliable [24]. More reliable is the detection of [Ne V] at 14 and 24 micron (MIR) [25] that suggests that the presence of AGN could be possibly 4 times higher than determined at optical wavelengths.

LINERs also pose interesting questions. If star formation and AGN are indeed interconnected (possibly with a time-delay due to AGN feedback quenching star formation [47]), then the fact that LINERs reside among old stars poses a puzzle. Maybe the once young and luminous stars present in an earlier Seyfert phase dim to a level where they can no longer be detected in contrast to the much brighter bulge population, especially when observed through large apertures. Again, the spatial resolution of GSGN, coupled to our sophisticated analysis techniques, will help identifying stellar population variations. Based on SDSS data, it was proposed [9] that LINERs containing true AGN show some residual level of recent star formation in the last Gyr, while those LINERs where stars are all old are not truly AGN, but retired galaxies [7], where the ionizing photon budget is dominated not by an AGN but hot post-AGB stars and white dwarfs. With the much greater sensitivity to AGN signatures of the GSGN will help disentangling true from fake AGN.

Our proposal: The Gemini Survey of Galactic Nuclei (GSGN). We propose a survey of galactic nuclei in the southern hemisphere inspired on the Palomar Survey. This will be, in fact the first such a survey of galaxies in the local universe done in the southern hemisphere. But it is not meant to replicate the Palomar Survey. First it is designed to go much deeper (although for a smaller sample): It will use an 8 m telescope (instead of 5 m) with updated detector technology. More importantly, it will be made with 3D spectroscopy instead of a single slit. It will have a spatial resolution limited by seeing instead of a single spectrum with 4"x2". In fact this survey will have the highest spatial resolution of any survey of galaxies done or in progress. The scientific goals of our survey are: ***a-Nuclear emission line properties.*** Detect and study the statistical, geometric and physical properties of Low Luminosity AGN (LLAGN): "dwarf" Seyferts and LINERs as well as starburst nuclei. We propose to carry out the deepest demographic study of supermassive black holes and their local environment yet performed. ***b-Circumnuclear emission line properties.*** We expect to determine the nature and ionization mechanism of the line emitting gas in the circum-nuclear region with a ~100 pc scale. We have found that in a few cases one can see the light of the AGN being reflected by the ionization cones [31, 36, 50, 51]. This is an additional demonstration of the existence of a central black hole. It also demonstrates the application of the unified model to LLAGN. These findings were made with the use of PCA tomography [30] and many more such configurations could be found in the survey [31]. Gaseous kinematics may also provide important information about the black hole mass and the geometry of the emitting region [52]. ***c-Stellar kinematical properties.*** This will allow to determine the mass of the black hole for the nearest massive galaxies as well as to recover important parameters as the existence of stellar discs and their angular momentum. We will determine the stellar parameters related to kinematics (Gauss-Hermite moments [26]). With those, it is possible to measure the angular momentum related parameter λ_R [28]. This is the parameter that defines, in combination with the eccentricity, slow and fast rotators. We intend to relate λ_R to other parameters such as galaxy morphology, galaxy stellar luminosity, AGN properties, galaxy environment (groups, clusters etc). For this purpose, we will use the Jeans [29] and the Schwarzschild methods. We will also determine the mass to light (M/L) ratio

whenever it is possible and correlate this with other parameters such as velocity dispersion [27] or IMF [28]. *d-Stellar population archeology*. Techniques to dissect the fossil record of star formation and chemical histories encoded in galaxy spectra have matured tremendously over the past decade. Both index-based and full spectral fitting methods have been perfected and used to explore the avalanche of data from surveys like the SDSS [32, 41-43], advancing our understanding of the global (spatially integrated) SFH of galaxies of different types. Stellar population models also developed significantly over the last years, making possible to estimate the time scale of the star formation history via the measurement of alpha-enhancements in integrated spectra [48, 49]. These stellar archeology techniques recently started to be applied to IFU-based surveys like ATLAS^{3D} and CALIFA [44, 45], producing SFH maps with \sim kpc scale resolution. Elaborated pipelines have been devoted to explore the highly informative manifold resulting from combination of the spatial information with the age/chemical abundances/extinction record [46].

References

- 1- Ho, L. C. 2008, ARAA, 46, 475
- 2- Heckman, T.M., 1980, A&A, 87, 152
- 3- Ferland, G.J., Netzer, H., 1983, ApJ, 105, 113
- 4- Halpern, J.P, Steiner, J.E., 1980, ApJ, 269, L37
- 5- Phillips, M.M., Jenkins, C.R., Dopita, M.A., Sadler, E.M., Binette, L., 1986, AJ, 91, 1062
- 6- Binette, L., Magris, C., Stasinska, G., Bruzual, A. G., 1994, A&A, 292, 13
- 7- Stasinska, G et al, 2008, MNRAS, 391, L29
- 8- Eracleous, M., Hwang, J.A., Flohic, H.M.L.G., 2010, ApJ, 187, 796
- 9- Cid Fernandes, R., Stasinska, G., Mateus, A, Asari, N.V., 2011, MNRAS, 413, 1687
- 10- Yan, R., Blanton, M.R., 2012, ApJ, 747, 61
- 11- Walcher, J et al, 2006, ApJ 692
- 12- Bekki, K. and Graham, A. 2010 ApJ Lett 714, L31
- 13- Neumayer, N. and Walcher, J. 2012 Adv Astron Vol. 2012
- 14- Ferrarese, L. & Merritt, D. 2000, ApJ, 539, L9
- 15- Gebhardt, K., et al. 2000, ApJ, 539, L13
- 16- Gultekin, K., et al. 2009, ApJ, 698, 198
- 17- Springel, V., Di Mateo, T. & Hernquist, L. 2005, MNRAS, 361, 776
- 18- Hopkins, P. F. & Hernquist, L. 2006, ApJS, 166, 1
- 19- Granato, G. L., de Zotti, G., Silva, L., Bressan, A. & Danese, L. 2004, ApJ, 600, 580
- 20- Filippenko, A & Sargent, W 1985, ApJ Supp 57,503
- 21- De Zeeuw, T et al 2002 MNRAS 329, 513
- 22- Cappellari et al 2011 MNRAS 413, 813
- 23- Sanchez et al 2012, AA 538,8
- 24- Desroches, L-B. & Ho, L. C. 2009, ApJ 690, 267
- 25- Satyapal et al 2008 ApJ 677
- 26- Cappellari, M. & Emsellem, E. 2004, PASP, 116, 138 (pPXF)
- 27- Cappellari, M et al 2006 MNRAS 366, 1126
- 28- Cappellari, M. et al. 2012 Nat 484, 485
- 29- Cappellari, M., 2008, MNRAS, 390, 71
- 30- Steiner, J. E., Menezes, R. B., Ricci, T. V. & Oliveira, A. S. 2009, MNRAS, 395, 64
- 31- Ricci, T. V., Steiner, J. E. & Menezes, R. B. 2011, ApJ, 734, L10
- 32- Cid Fernandes, R., Mateus, A, Sodré Jr, L. et al 2005, MNRAS, 358, 363
- 33- Sandage, A. & Tammann, G. A. 1981, A Revised Shapley-Ames Catalog of Bright Galaxies. Washington, DC: Carnegie Inst. Wash.
- 34- Kormendy, J. & Kennicutt, R. C. 2004, ARAA, 42, 603
- 35- Kormendy, J & Ho, L.C. 2013, ARAA
- 36- Menezes, R. B. 2012 - Phd Thesis – Universidade de São Paulo
- 37- Steiner J. E. et al 2009 MNRAS 396, 788
- 38- Heckman et al (1997), ApJ 482, 114
- 39- Cid Fernandes et al (2001) Ap J 558, 81

- 40- González Delgado et al (2001) ApJ 546, 845
- 41- Kauffmann et al (2003) MNRAS 346, 1055
- 42- Gallazzi et al (2005) MNRAS 362, 41
- 43- Vale-Asari et al (2009) MNRAS 396, L71
- 44- McDermid 2013 arXiv 1211.2317
- 45- Pérez et al 2013 ApJ 764, L1
- 46- Cid Fernandes et al 2013 A&A 557, 86
- 47- Wild et al 2010 MNRAS 405, 933
- 48- Thomas et al 2005, ApJ 621, 673
- 49- Walcher et al 2009 MNRAS 398, 44 M
- 50- Menezes, R. B., Steiner, J. E., Ricci, T. V. 2013 Ap J 765, L40
- 51- Ricci, T, V 2013 PhD Thesis Universidade de São Paulo
- 52- Menezes, R. B., Steiner, J. E. & Ricci, T. V. 2013 Ap J 762, L29

Experimental Design

The **SAMPLE**: From a Log N-Log S type of argument one can show that the Revised Shapley-Ames Catalog of Bright Galaxies [33] is nearly complete to $B=12.4$. At $B=12.5$ the degree of incompleteness starts to be significant. It is also clear that the sample is complete to $|b|>15^\circ$. For the sample to be feasible in the LLP program we have chosen all galaxies with $B<12.0$, $\delta<0^\circ$ and $|b|>15^\circ$. This sample has a total of 181 galaxies. From them, 11 are Sm/Im in which one cannot identify a nucleus in the 2MASS images. The total number of our sample is therefore 170 galaxies. A sub-sample of 36 massive galaxies ($\sigma>200$ km/s) have already been allocated time in 2013. In addition, 7 galaxies have already been observed in other programs (NGC 253-300-908-1068-1313-1566-7424). Why a sample limited to $B=12.0$ and not to any other limit? In surveys like this, the larger the sample, more accurate the conclusions. With the limit of $B=12.0$ our uncertainties will be of $\sim 7.4\%$. With a limit of $B=12.5$ the accuracy would increase to 5.2% but it would cost twice as much telescope time, and would not be feasible within the limits of our LLP program. **The STRATEGY**: The remaining 127 galaxies demand about 135 hours of observations, considering that on average each galaxy needs 1.06 hs of telescope in order to achieve S/N ~ 10 per fiber. We propose to complete the GSGN survey in 8 semesters, requiring about 17 hours per semester (see Table 1 and technical description). We will use a strategy of prioritizing 5 sub-samples of galaxies: a- The massive galaxy (MG), with $\sigma>200$ km/s. This comprises a total of 36 galaxies. b- Early type (ETG) – galaxies of morphologies E+S0. c- All LTG (late type galaxies) with $B<11.5$. We will call this the Sc sub-sample. d -All LTG to $B=12.0$. e - All other galaxies.

The GSGN is LEGACY project. As in the standard Gemini procedure, all data will be available to international access as soon as the proprietary period is over. More than that, we will offer all our reduced and processed data cubes to the Brazilian community, by request, 6 months after each of the subsample processing has been completed. For each galaxy the fully reduced and processed data cube will be available. This means that we will have 170 data cubes with 4800 spectra each. The total of 700 thousand fully processed spectra will be made available to the Brazilian community. The GSGN team comprises experts in all areas related to this field, from stellar libraries and evolutionary tracks (major ingredients in the analysis of stellar populations) to spectral fitting, emission lines, sophisticated data reduction and analysis tools, as well as the organization and distribution of data and value added products in public databases. After the reduction, a data treatment will be applied with the following routines, all developed and validated by our group [36]: DAR correction; Butterworth filtering of spatial and spectral high frequency noises; removal of instrumental fingerprints; R-L deconvolution. The data will be analyzed with the following techniques: PCA Tomography [30, 31]; determination of the stellar Gauss-Hermite moments with the pPXF procedure [26]; stellar spectral synthesis [32] and archeology; analysis of the residual emission lines, after the stellar continuum subtraction

with traditional diagnostic diagrams [19]. In addition we will also test a new method to detect AGN, associated with high and low density clouds [37].

The proponent's responsibilities: **Joao Steiner** (coordination); **Roberto Cid Fernandes** (Methods of spectral synthesis; stellar archeology); **Paula Coelho** (study and definition of stellar template basis; stellar archeology); **Natalia Vale Asari** (analysis of objects with faint emission lines/retired galaxies; dust diagnostics; emission line modeling); **Roberto B. Menezes**, **Tiago V. Ricci and Daniel May** (Interaction with the Gemini Observatory; data reduction; data processing: DAR correction, fingerprint removal, Butterworth filtering, deconvolution, PCA Tomography; starlight spectral synthesis; emission line analysis); analysis and modeling of stellar kinematics; **André Luiz de Amorim** (Database; analysis tools).

Please note that for 2014A we are submitting two related projects, with a total of 17 hs (Table 1). The accompanying project of Sc galaxies (Menezes et al) is being re-submitted as it has already been initiated. Even if our LLP project is not approved, it makes sense to be continued.

Technical justification

All of the observations will be performed with the GMOS-IFU in the single slit mode. The early-type galaxies will be observed using the B600 grating, in a central wavelength of 5620 Å. Such configuration provides a spectral coverage from 4250 Å to 7000 Å and a spectral resolution of 3.3 Å at 5620 Å. We require this spectral coverage in order to detect emission lines like H β , [O III] λ 4959; 5007, [O I] λ 6300, [N II] λ 6548; 6584, H α and [S II] λ 6716; 6731, which are considerably important for our purposes. We propose to obtain three observations, of 10 min integration each, of each one of the early-type galaxies. The late-type galaxies will be observed using the R831 grating, in a central wavelength of 5850 Å. Such configuration provides a spectral coverage from 4800 Å to 6890 Å and a spectral resolution of about 1.3 Å at 5850 Å. We require a higher spectral resolution in the observations of the late-type galaxies because many of them show significantly low values of the stellar velocity dispersions; therefore, a high spectral resolution is required in order to measure this kinematical parameter. We propose to obtain three observations, of 15 min integration each, of each one of the late-type galaxies.

Using the GMOS ITC for our faintest early-type galaxy (NGC 1700), whose source is an elliptical galaxy with 16.71 Bmag/arcsec² on the central region. The medium signal to noise is about 26 in this case. On the other hand, using the GMOS Integration Time Calculator for our faintest late type galaxy (NGC 5584), we concluded that it is possible to obtain a median S/N of about 10, except at wavelengths corresponding to the main emission lines, where the S/N is considerably higher. The surface brightness (an input parameter for the ITC) was calculated by taking the flux of the central region of NGC 1042 corresponding to the field of view of the IFU (17.5 square arcsec) as being equal to, approximately, 9% of the total flux of the galaxy. This flux fraction was estimated using an HST image of this galaxy. Our previous experiences revealed that our methods of analysis require a minimum S/N of about 10 in order to provide reliable information.

We propose to obtain an arc lamp observation for each target. Considering, for the early-type galaxies, a 18 min telescope setup time per target plus a 1.5 min exposure corresponding to the observation of the arc lamp image plus 76 s per exposure to cover the readout time, we estimate that, for each early-type galaxy, it is necessary an integration time of 18 min + 3*(10) min + 3*76 s + 1.5 min + 76 s = 54.57 min = 0.91 hr. On the other hand, considering, for the late-type galaxies, a 18 min telescope setup time per target plus a 5 min exposure corresponding to the observation of the arc lamp image plus 76 s per exposure to cover the readout time, we estimate that, for each late-type galaxy, it is necessary an integration time of 18 min + 3*(15) min + 3*76 s + 5 min + 76 s = 73.07 min = 1.22 hr.

Since our sample comprises 62 early-type galaxies and 58 late-type galaxies, we require a total of $62 \times 0.91 \text{ hr} + 58 \times 1.22 \text{ hr} = 127.18 \text{ hr}$ to complete the program. We require the following observing conditions: Sky Background = 80%, Cloud Cover = 70%, Image Quality = 70% and Water Vapor = Any. Under these conditions, which correspond to 39.2% of all observing nights, no target in the 2014 A semester has a probability of finding guiding stars lower than 33%. Since we do not require specific position angles for the observations, the probabilities of finding guiding stars lower than 100% obtained with the Phase I Tool will probably not represent problems for the observations.

Table 1: The requested time, per semester

| | MG | Sc (B<11.5) | GSGN |
|-------------|--------|-------------|----------------|
| 2013A | 14.1hs | 2.5 hr | |
| 2013B | 12.3hs | 3.9 hs | |
| 2014A | | 10.4 hs | 6.6 hs |
| 2014B | | | 17 hs |
| 2015A-2017B | | | 17 hs/semester |

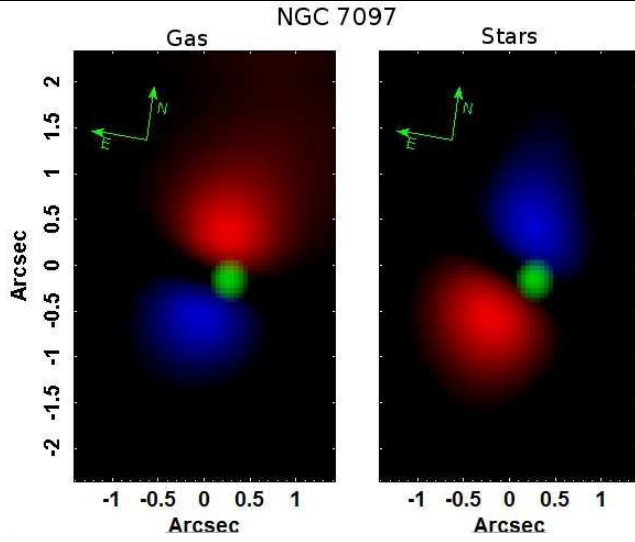


Figure 1 – Tomograms (see [30, 51] for definitions) of NGC 7097 representing the counter rotating gaseous and stellar disks (blue and red) as well as the AGN (green).

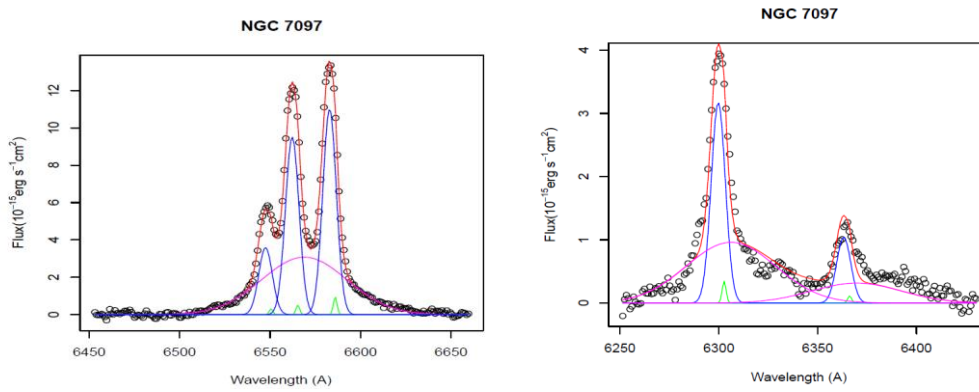


Figure 2. Left: Gaussian decomposition of the H α /[N II] lines, showing the broad and narrow components. Right: The same for the [O I] lines showing again the broad (surprising!) and narrow components.